Journal of Atmospheric and Solar-Terrestrial Physics 105-106 (2013) 231–244

Contents lists available at ScienceDirect

Journal of Atmospheric and Solar-Terrestrial Physics

journal homepage: www.elsevier.com/locate/jastp

Plasma modifications induced by an X-mode HF heater wave in the high latitude *F* region of the ionosphere

N.F. Blagoveshchenskaya[a,*], T.D. Borisova[a], T.K. Yeoman[b], M.T. Rietveld[c], I. Häggström[d], I.M. Ivanova[a]

[a] Arctic and Antarctic Research Institute, Petersburg, Russia
[b] Department of Physics and Astronomy, University of Leicester, LEI 7RH, UK
[c] EISCAT Scientific Association, Ramfjordbotn, Norway
[d] EISCAT Scientific Association, Kiruna, Sweden

ARTICLE INFO

Article history:
Received 4 April 2012
Received in revised form
25 September 2012
Accepted 9 October 2012
Available online 23 October 2012

Keywords:
Ionosphere (Active experiments) – Radio Science (Nonlinear phenomena)

ABSTRACT

We presented experimental results of strong plasma modifications induced by X-mode powerful HF radio waves injected towards the magnetic zenith into the high latitude *F* region of the ionosphere. The experiments were conducted in 2009–2011 using the EISCAT Heating facility, UHF incoherent scatter radar and the EISCAT ionosonde at Tromsø, Norway; and the CUTLASS SuperDARN HF coherent radar at Hankasalmi, Finland. The results showed that the X-mode HF pump wave can generate strong small-scale artificial field aligned irregularities (AFAIs) in the *F* region of the high-latitude ionosphere. These irregularities, with spatial scales across the geomagnetic field of the order of 9–15 m, were excited when the heater frequency (f_H) was above the ordinary-mode critical frequency (*foF*2) by 0.1–1.2 MHz. It was found that the X-mode AFAIs appeared between 10 s and 4 min after the heater is turned on. Their decay time varied over a wide range between 3 min and 30 min. The excitation of X-mode AFAIs was accompanied by electron temperature (*Te*) enhancements and an increase in the electron density (*Ne*) depending on the effective radiated power (ERP). Under ERPs of about 75–180 MW the *Te* enhances up to 50% above the background level and an increase in *Ne* of up to 30% were observed. Dramatic changes in the *Te* and *Ne* behavior occurred at effective radiated powers of about 370–840 MW, when the *Ne* and *Te* values increased up to 100% above the background ones. It was found that AFAIs, *Ne* and *Te* enhancements occurred, when the extraordinary-mode critical frequency (*fxF*2) lied in the frequency range $f_H - f_{ce}/2 \le fxF2 \le f_H + f_{ce}/2$, where f_{ce} is the electron gyrofrequency. The strong *Ne* enhancements were observed only in the magnetic field-aligned direction in a wide altitude range up to the upper limit of the UHF radar measurements. In addition, the maximum value of *Ne* is about 50 km higher than the *Te* enhancement peak. Such electron density enhancements (artificial ducts) cannot be explained by temperature-dependent reaction rates. They can be attributed to HF-induced ionization production by accelerated electrons. The possible mechanisms for plasma modifications induced by powerful X-mode HF radio waves were discussed.

1. Introduction

Powerful High Frequency (HF) radio waves transmitted from high-power ground-based HF heating facilities could strongly modify the ionospheric plasma. A wide variety of phenomena are observed in the *F* region of the ionosphere near the reflection altitude of powerful HF radio waves with ordinary polarization (O-mode). This is due to the fact that in the vicinity of a plasma resonance these waves effectively interact with the ionospheric plasma, resulting in the growth of thermal parametric (resonance) and parametric decay instabilities (Vas'kov and Gurevich, 1976; Grach and Trakhtengerts, 1976; Stubbe, 1996; DuBois et al., 1990; Gurevich, 2007). These instabilities and mode conversions, driving Langmuir and upper hybrid turbulence, lead to intense plasma oscillations, an increase in the electron temperature, the excitation of small-scale artificial field-aligned irregularities (AFAIs) and stimulated electromagnetic emission, the acceleration of electrons, which, in turn, leads to the artificial optical emission from the perturbed ionosphere and artificial plasma ionization.

Among the phenomena discovered from ionospheric modification experiments one of the most outstanding is the excitation of small-scale artificial field-aligned irregularities (AFAIs) or striations. Their maximum spatial scale across the magnetic field is determined by the quantity $l = c/f_H$, where f_H is the heater frequency and c is the speed of light. For example, for $f_H = 5$ MHz, l amounts to 60 m. The size of AFAIs along the magnetic field line

* Corresponding author. Tel.: +7 812 337 3191; fax: +7 812 352 2688.
E-mail address: nataly@aari.nw.ru (N.F. Blagoveshchenskaya).

1364-6826 © 2012 Elsevier Ltd. Open access under CC BY license.
http://dx.doi.org/10.1016/j.jastp.2012.10.001

is determined by the length of the electron heat conduction and can reach 30–50 km. AFAIs have been excited through a large number of experiments at a variety of HF heating facilities located at mid and high latitudes (Minkoff et al., 1974; Hedberg et al., 1983; Djuth et al., 1985; Noble et al., 1987; Kelley et al., 1995; Hysell et al., 1996; Frolov et al., 1997; Yeoman et al., 2007; Yampolski et al., 1997; Robinson et al., 1997;1998; 2006; Eglitis et al., 1998; Honary et al., 1999; Rietveld et al., 2003; Blagoveshchenskaya et al., 1998; 2001; 2006; 2009). They occur at the upper hybrid resonance altitude when ordinary (O-mode) polarized HF pump waves reach the ionospheric reflection height. An O-mode HF pump wave couples through striations into electrostatic (upper hybrid) waves at the upper hybrid resonance altitude, where the heater frequency is $f_H{}^2 = f_{UH}{}^2 = f_p{}^2 + f_{ce}{}^2$, here f_p is the local plasma frequency and f_{ce} is the electron gyrofrequency. The upper hybrid resonance height is typically several kilometers below the reflection level of the HF pump wave. Upper hybrid waves propagate in a direction near perpendicular to the magnetic field and their energy dissipation heats the electrons. Through the thermal parametric (resonance) instability (Grach and Trakhtengerts, 1976; Vas'kov and Gurevich, 1976), these waves can excite AFAIs which can trap the excited upper hybrid field. Thermal parametric instability develops when an O-mode high-power HF radio wave is reflected from the ionosphere, $f_H^2 = f_p^2$.

The HF pump waves with O-mode polarization have been almost always used in the modification experiments in the ionosphere *F* region. An extraordinary polarization (X-mode) HF pump wave is reflected at the altitude having a plasma frequency $f_p^2 = f_H (f_H - f_{ce})$, that is below the reflection altitude and the upper hybrid resonance level of the ordinary polarization (O-mode) HF pump wave. Since the resonance altitude in the ionosphere cannot be reached by an extraordinary polarization (X-mode) HF pump wave transmitted from the ground, only O-mode waves can excite striations. Frolov et al. (1999) have found that the additional X-mode heating may produce the modification of effects induced by an O-mode powerful wave. As a rule, X-wave modification results in the suppression of the stimulated electromagnetic emission (SEE) generation for different spectral components and the suppression of the intensity of artificial small-scale irregularities. The observations of O- and X-mode heating effects observed simultaneously with the SuperDARN (Super Dual Auroral Radar Network, Greenwald et al., 1995) CUTLASS (Co-operative UK Twin Located Auroral Sounding System, Lester et al., 2004) and EISCAT (European Incoherent Scatter, Rishbeth and Van Eyken, 1993) radars reported by Robinson et al. (1997) clearly demonstrated evidence of heater-induced striations in the *F* region ionosphere using CUTLASS backscatter power data only during O-mode heating. Similarly, the electron temperature enhancements seen in the Tromsø EISCAT UHF radar data were also observed only during O-mode heating. It is significant that, during the observations, the heater frequency was less than the ordinary-mode critical frequency of the *F*2 layer, $f_H < foF2$. This indicates that the O-mode HF pump wave was certainly reflected from the ionosphere and the thermal parametric (resonance) instability was excited at the upper hybrid resonance altitude.

Blagoveshchenskaya et al. (2011a, 2011b) presented the first experimental evidence of the excitation of strong small-scale AFAIs, with spatial scales across the geomagnetic field of the order of $l_\perp \approx$ 9–15 m, in the high-latitude *F* region of the ionosphere due to an X-mode HF pump wave, radiated towards the magnetic zenith. Their generation requires X-mode *F* region modification at frequencies, $f_{H,}$ which are above the ordinary-mode critical frequency, *foF*2, by 0.3–0.4 MHz. At the same time f_H lies in the vicinity of the extraordinary component of critical frequency, $fxF2 \approx f_H > foF2$. The results obtained are new and interesting, but they were founded on a limited number of experiments.

In this paper, we primarily focus on plasma modification associated with small-scale artificial field-aligned irregularities and on the behavior of the plasma, when the high-latitude ionosphere *F* region is affected by an X-mode high-power HF radio wave at frequencies above the ordinary-mode critical frequency. We present and discuss behavior, features and conditions of generation of X-mode AFAIs from numerous experiments carried out under different heater frequencies and background geophysical conditions. The electron temperature *Te* and density *Ne* enhancements are studied in detail for different effective radiated power (ERP=75–180 MW and ERP=370–840 MW). We hope that unexpected strong heater-induced phenomena, occurring in the *F* region under X-mode heating, will provide motivation for new investigations. The study is based on a large number of experiments performed by the Arctic and Antarctic Research Institute in the course of five Russian EISCAT heating campaigns from 2009–2011. The structure of the paper is as follows. Experimental setup is explained in Section 2, followed by observational results (Section 3), which are discussed in detail in Section 4. Observations and main results are summarized in Section 5.

2. Experimental arrangement

The experiments reported here were conducted in the course of five Russian EISCAT heating campaigns from November 2009, March and November 2010, and March and October 2011 in the evening hours from 14 to 17 UT. The EISCAT HF heating facility (Rietveld et al., 1993) located near Tromsø in Northern Norway (geographical coordinates 69.6°N, 19.2°E; magnetic dip angle $I = 78°$) was used to modify the ionosphere in the high-latitude *F* region. In the course of the experiments from November 2009, March and November 2010, and March 2011 phased array 2 (3.9–5.5 MHz) was used, resulting in an effective radiated power (ERP) of 75–180 MW. The width of the HF antenna beam at the - 3 dB point was 12°–14° depending on the heater frequency. The heating facility operated at 3.95, 4.04, 4.9128, and 5.423 MHz, with X-mode polarization, and with 10 min continuous HF pulses. Phased array 1 (5.4–8 MHz), with the width of the HF antenna beam of about 6°, was used in October 2011, resulting in an effective radiated power (ERP) of 340–840 MW. The heating facility operated at 5.423, 6.77, 7.1, and 7.953 MHz, also with X-mode polarization, and with 10 min continuous HF pulses. The HF heater antenna beam was tilted 12° to the south of zenith, thus allowing HF pumping in the field-aligned direction (magnetic zenith, MZ).

The modified ionospheric *F* region was probed by the CUTLASS Hankasalmi, Finland radar (63°N, 27°E). CUTLASS is a pair of HF coherent backscatter radars located in Finland and Iceland and forms part of the SuperDARN array (Greenwald et al., 1995; Lester et al., 2004). The CUTLASS (Finland) radar transmitter site is located approximately 1000 km south of the Tromsø heating facility. The CUTLASS radar beam is approximately 3.3° wide and can dwell on 16 independent adjacent positions. In the course of the experiments described below, one beam position centered on the Tromsø heater (beam 5) was utilized. The CUTLASS (Finland) radar operated in all experiments when phased array 2 of Tromsø HF heater was utilized. In the course of the experiments of October 2011, when phased array 1 of Tromsø HF heater was utilized, the CUTLASS (Finland) radar did not operate.

The HF heating facility at Tromsø is located adjacent to the EISCAT UHF incoherent radar which operates at a frequency of 930 MHz (Rishbeth and Van Eyken, 1993). During the experiments the UHF radar measured the ionospheric plasma parameters, such as the electron density and temperature (*Ne* and *Te*), the ion temperature (*Ti*), and the ion velocity (*Vi*), in the altitude range from 90 to 600 km in the direction of the magnetic zenith. Ionograms were taken every four minutes using the EISCAT dynasonde, which is co-located with both the EISCAT UHF and heater array at Tromsø. The viewing geometry is shown in Fig. 1.

3. Observational results

3.1. Excitation of artificial small-scale field-aligned irregularities

Table 1 describes the heater and ionosphere parameters for the experiments on 5 and 6 November 2009, on 5, 6, and 8 March 2010, on 4, 5, 6, 7, and 10 November 2010, and on 5 and 6 March 2011 during which the ionosphere was modified by X-mode HF pump waves. The experiments were carried out during quiet magnetic conditions with the exception of 5 and 6 March 2011.

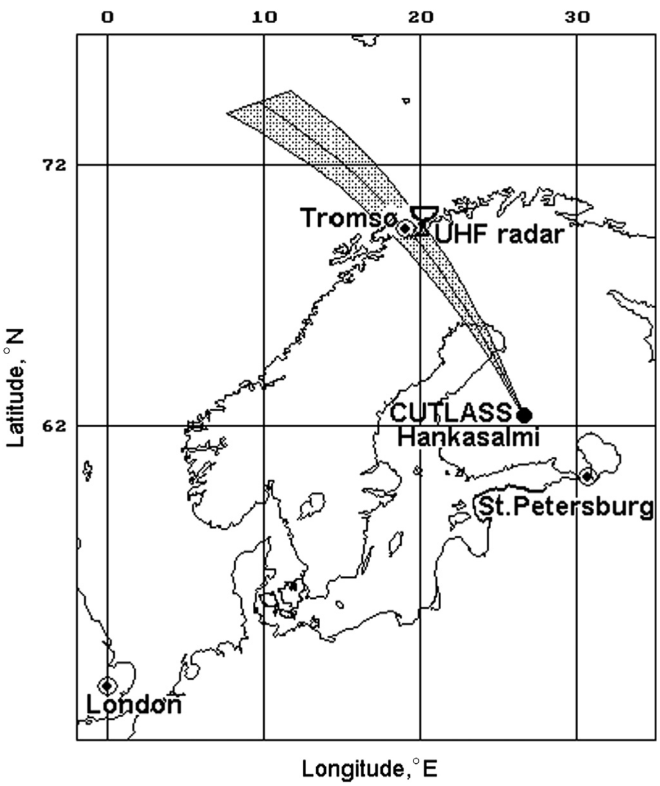

Fig. 1. Map showing the location of the EISCAT/Heating facility and the EISCAT UHF incoherent scatter radar, the viewing geometry of the CUTLASS Hankasalmi (Finland) HF coherent scatter radar.

In all of the above cases listed in Table 1 the excitation of strong AFAIs was observed from the CUTLASS Hankasalmi, Finland radar. The Tromsø ionosonde data indicated a smooth F2 layer with the critical frequency *foF*2 below the heater frequency, $f_{H,}$ by 0.1–1.2 MHz. In some heater-on sessions weak sporadic *E* layers with critical frequencies about of $foEs \approx 1.5$–2.8 MHz can be seen on the ionograms.

Experiments on 5 and 6 November 2009 (case 1 and 2 in Table 1) were the first to show the possibility of excitation the small-scale artificial field-aligned irregularities (AFAIs) induced by HF pump wave with X-mode polarization. They were observed by the CUTLASS Hankasalmi radar.

Fig. 2 illustrates the CUTLASS Hankasalmi backscatter power for a beam position centered on the Tromsø heater (beam 5) during the experiment on 6 November 2009 from 14:00 to 15:20 UT. The CUTLASS radar operated at a frequency of about 10 MHz and was therefore sensitive to small-scale field-aligned irregularities with the spatial size across the geomagnetic field of the order of $l_\perp \approx 15$ m ($l_\perp = \lambda/2$, where λ is the wave length of radar). The CUTLASS Hankasalmi radar was operating in a standard mode with 45 km range gates with the first range-gate starting at 180 km. Range-gate 17 corresponds to the center of the heated patch above Tromsø. For O-mode heater effects in the first two heater-on periods the HF pump wave with O-mode of polarization was radiated towards the magnetic zenith. As can be seen from Fig. 2 , the signals scattered from AFAIs were absent. Here the heater frequency $f_H = 3.95$ MHz was above the critical frequency of *F*2 layer ($foF2 \approx 3.5$ MHz) and AFAIs cannot be generated. In the next heater-on cycle from 14:31 to 14:41 UT, when *foF*2 decreased to 3.3–3.4 MHz, the polarization of HF pump wave was changed from O- to X-mode. The polarization change of the heater wave corresponds to the appearance of intense scattered signals above Tromsø. In this experiment a power stepping mode, utilizing an orderly sequence of 20%, 50%, 70%, 85%, 100%, 100%, 85%, 70%, 50%, 20% (from 30 to 157 MW and back) was used. The duration of each step is 1 min. AFAIs appeared under 50% effective radiated power (ERP $\approx$ 75 MW) and reached their maximum at full ERP. The decrease of ERP from 100% to 20% in the second part of the heater-on cycle did not

Table 1
List of the EISCAT Heating experiments when the X-mode AFAIs were excited in the *F* region of the high latitude ionosphere with the use of phased array 2.

N	Date	Time of observations, (UT)	Total number of "ON" cycles	f_H, (MHz)	ERP, (MW)	*foF*2, (MHz)	*foEs*, (MHz)
1	5.11.09	14:45–15:30	1	3.95	126	3.3	1.8
2	6.11.09	14:26–15:20	1	4.040	power stepping from 30 to 157	3.3	–
3	5.03.10	15:30–17:00	3	4.9128	123	4.2–3.7	2.0
4	6.03.10	15:55–17:00	3	4.9128	115	4.4–4.2	–
5	8.03.10	16:00–17:00	4	5.423	123–100	4.8	–
6	4.11.10	14:30–15:00	2	4.9128	173	3.9–3.8	2.8–2.6
7		15:05–15:30	2	4.544	109	3.8–3.6	2.8–2.2
8	5.11.10	14:05–15:00	4	4.9128	145	4.6–3.9	2.0–1.6
9		15:05–16:15	5	4.040	112	3.9–3.4	2.0
10	6.11.10	13:50–14:50	4	4.544	95	4.2–3.6	–
11		14:55–17:00	6	4.040	117	3.6–3.0	2.1
12	7.11.10	13:50–15:15	6	4.544	85	4.2–3.4	1.6
13		15:20–16:15	4	4.040	114	3.4–3.1	1.6
14	10.11.10	13:35–15:00	6	4.544	113	4.5–3.6	2.8–1.6
15		15:05–16:35	6	3.95	151	3.6–3.0	1.6–2.1
16	5.03.11	16:35–17:15	3	4.544	112	4.0–3.5	–
17	6.03.11	16:05–16:30	2	4.544	75	4.3–3.5	1.5
18		16:35–17:15	2	3.95	106	3.5–2.7	1.5–2.0

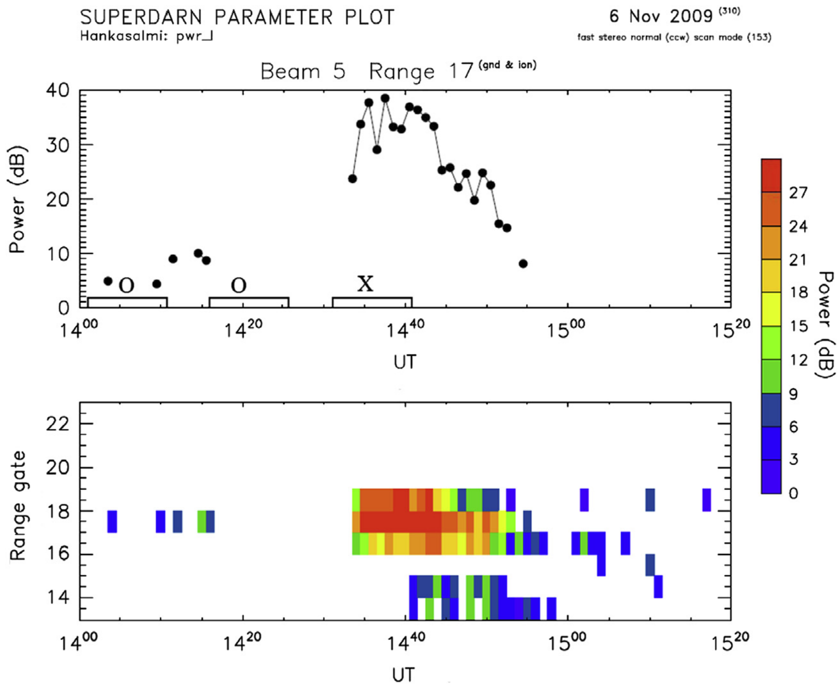

Fig. 2. Backscattered power from the Hankasalmi (Finland) CUTLASS radar (beam 5) at operational frequency of about 10 MHz for contrasting O/X-mode heating on 6 November, 2009 between 14:00 and 15:20 UT. Behavior of the backscattered power in gate 17, corresponding to the central part of the heated patch, is shown in the top panel and its behavior in the range-gate –universal time UT coordinates is given in the bottom panel. Power stepping mode of the Tromso HF heating facility, utilizing an orderly sequence of 20%, 50%, 70%, 85%, 100%, 100%, 85%, 70%, 50%, 20% (from 30 to 157 MW and back) was used. The duration of each step is 1 min. The HF pump wave was radiated at a frequency of 4.04 MHz towards magnetic zenith. O/X-mode heater-on periods are marked on the top panel on the time axis.

affect the intensity of signals scattered from AFAIs. Moreover, their intensity remained constant during the first 5 min after the heater was turned off. Their decay time extends up to 15 min (see the top panel in Fig. 2).

In the course of the experiments on 5, 6 and 8 March 2010 (cases 3–5 in Table 1) the CUTLASS Hankasalmi radar was running a non-standard mode optimized for the observations of heating effects over Tromsø with one fixed beam (beam 5) with a high temporal and spatial resolution. It operated almost simultaneously at three frequencies of ~10, 13 and 17 MHz and was therefore sensitive to AFAIs with the spatial size across the geomagnetic field of the order of $l_\perp \approx 15$, 11, and 9 m. The temporal resolution of 1 s and 15 km range gates, with the first gate starting at a range of 480 km, were utilized.

Similar to the experiments on 5 and 6 November 2009, before X-mode heating the HF pump wave with O-mode polarization was radiated in experiments on 5 and 6 March 2010. The polarization of the HF pump wave was changed from O- to X-mode when the O-mode AFAIs disappeared and the heater frequency $f_H = 4.9128$ MHz became above the critical frequency of *F*2 layer by 0.5–0.7 MHz (*foF*2 = 4.2–4.4 MHz). The polarization change of the heater wave produced scattered signals over Tromsø. For brevity, the data are not presented here, but on 6 March 2010 the scattered signals were observed at three CUTLASS frequencies 10, 13, and 17 MHz, corresponding to the spatial scale of artificial irregularities $l_\perp \approx 15$, 11, and 9 m. The excitation of AFAIs with different spatial scales, responsible for the CUTLASS backscatter, occurred in all three heater-on periods. The results of the experimental observations on 5 March 2010 are very similar to the case of 6 March 2010 but in this experiment only AFAIs with $l_\perp \approx 15$ and 11 m were excited. In the course of the experiment on 8 March 2010 the HF pump wave was radiated at frequency of $f_H = 5.423$ MHz. It was the only experiment, from all those listed in Table 1, when O-mode heating at the same frequency was not carried out prior to the X-mode heating. Nonetheless during the experiment on 8 March 2010 the AFAIs with different spatial sizes of $l_\perp \approx 15$, 11 and 9 m were excited in four consecutive 10 min heater-on periods when the HF pump wave with X-mode polarization was radiated in the direction of magnetic zenith.

A rich variety of experiments have been carried out on 4, 5, 6, 7, and 10 November 2010 (see cases 6–15 in Table 1). In the course of experiments in the evening hours the electron density in the *F* region dropped, and the heater frequency was chosen so that f_H exceeded the value of *foF*2 by 0.1–1.2 MHz. This allows the study of the behavior of X-mode AFAIs for different relations between f_H and *foF*2. Similar to the experiments of March 2010, the CUTLASS Hankasalmi radar was also running a non-standard mode optimized for the observations of heating effects over Tromsø with one fixed beam (beam 5). It operated almost simultaneously at three frequencies of ~10, 11.5 and 13 MHz and was therefore sensitive to AFAIs with the spatial size across the geomagnetic field of the order of $l_\perp \approx 15$, 13, and 11 m.

Fig. 3 shows the CUTLASS Hankasalmi backscatter power at three frequencies of ~10, 11.5 and 13 MHz for a beam position centered on the Tromsø heater (beam 5) during the experiment on 6 November 2010 from 13:32 to 15:00 UT. Similar to the previous experiments of November 2009 and March 2010, before X-mode heating, the HF pump wave with O-mode polarization was radiated. In the second part of the heater-on period from 13:35–13:45 UT, when the critical frequency of *F*2 layer was about *foF*2 ≈ 4.2 MHz, AFAIs began to decay. The polarization of the HF pump wave was changed from O- to X-mode in the next heater-on period from 13.50–14.00 UT. The polarization change of the heater wave produced scattered signals over Tromsø at three CUTLASS frequencies. On 6 November 2010 X-mode heating was performed during four consecutive heating cycles (see Table 1). The excitation of AFAIs with different spatial scales, responsible for the CUTLASS backscatter, occurred in all four heater-on periods when the critical frequency of *F*2 layer dropped from

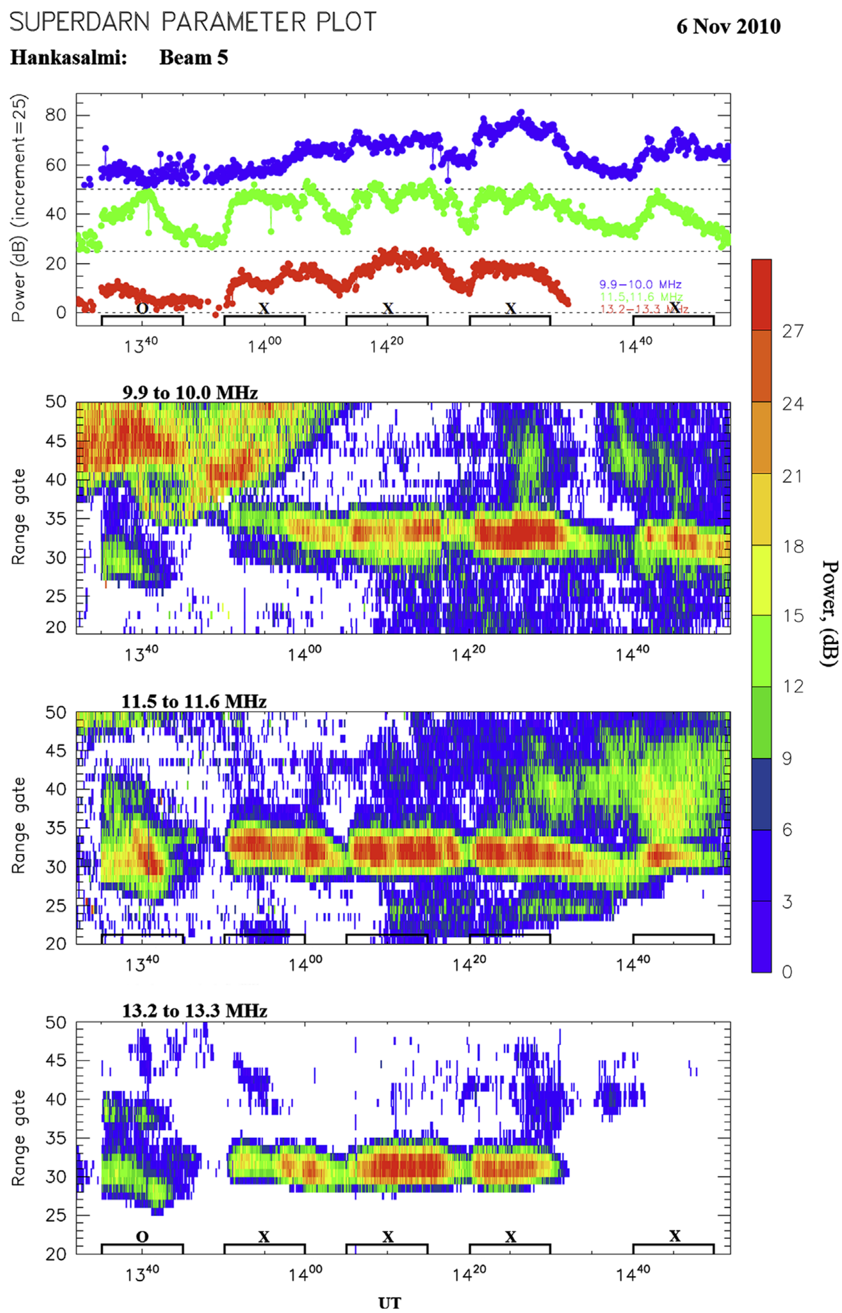

Fig. 3. Backscattered power from the Hankasalmi (Finland) CUTLASS radar (beam 5) at operational frequencies of about 10, 11.5 and 13 MHz during the experiment on 6 November 2010 from 13:32 to 15:00 UT. Behavior of the backscattered power averaged between 30–34 gates, corresponding to the central part of the heated patch, is shown in the top panel and its behavior in the range-gate –universal time UT coordinates is given in the bottom panels. HF pump wave was radiated at a frequency of 4.544 MHz towards magnetic zenith. Effective radiated power was about 180 MW. O/X-mode heater-on periods are marked on the top panel on the time axis.

4.2 to 3.6 MHz and the heater frequency f_H=4.544 MHz was above *foF*2 by 0.3–0.9 MHz. The most small-scale AFAIs with $l_\perp \approx 11$ m disappeared after the heater-on period from 14:20 to 14:30 UT. The CUTLASS backscattered signals at frequencies of ~10, 11.5 MHz were observed in the next heater-on period from 14:40–14:50 UT when the values of *foF*2 became about 3.6 MHz. The duration of heater-off period was 5 min with the exception of period from 14:30 to 14:40 UT when 10 min pause was used between heater-on cycles. It can be seen from Fig. 3 that X-mode AFAIs existed almost continuously, their decay time exceeded the duration of the heater-off periods (5 and 10 min). At 14:55 UT the heater frequency was changed to f_H=4.04 MHz. Again, the excitation of X-mode AFAIs occurred in all six heater-on periods when the critical frequency of *F*2 layer dropped from 3.6 to 3.0 MHz.

Experiments on 5 and 7 November 2010, again for brevity not presented here, are very similar to the experiment on 6 November 2010. They demonstrated the same features and behavior of X-mode AFAIs. There is some variation from the others in the experiment performed on 10 November 2010. In this event the polarization of the HF pump wave was changed from O- to X-mode when the heater frequency f_H=4.544 MHz was near the critical frequency of *F*2 layer *foF*2=4.5 and intense O-mode AFAIs with spatial scale of $l_\perp \approx 15$, 13, and 11 m were excited.

Fig. 4 illustrates the CUTLASS Hankasalmi backscatter power at three frequencies of ~10, 11.5 and 13 MHz for a beam position centered on the Tromsø heater (beam 5) during the experiment on 10 November 2010 from 13:18 to 15:12 UT. It is seen from Fig. 4 that the change of polarization of the heater wave produced

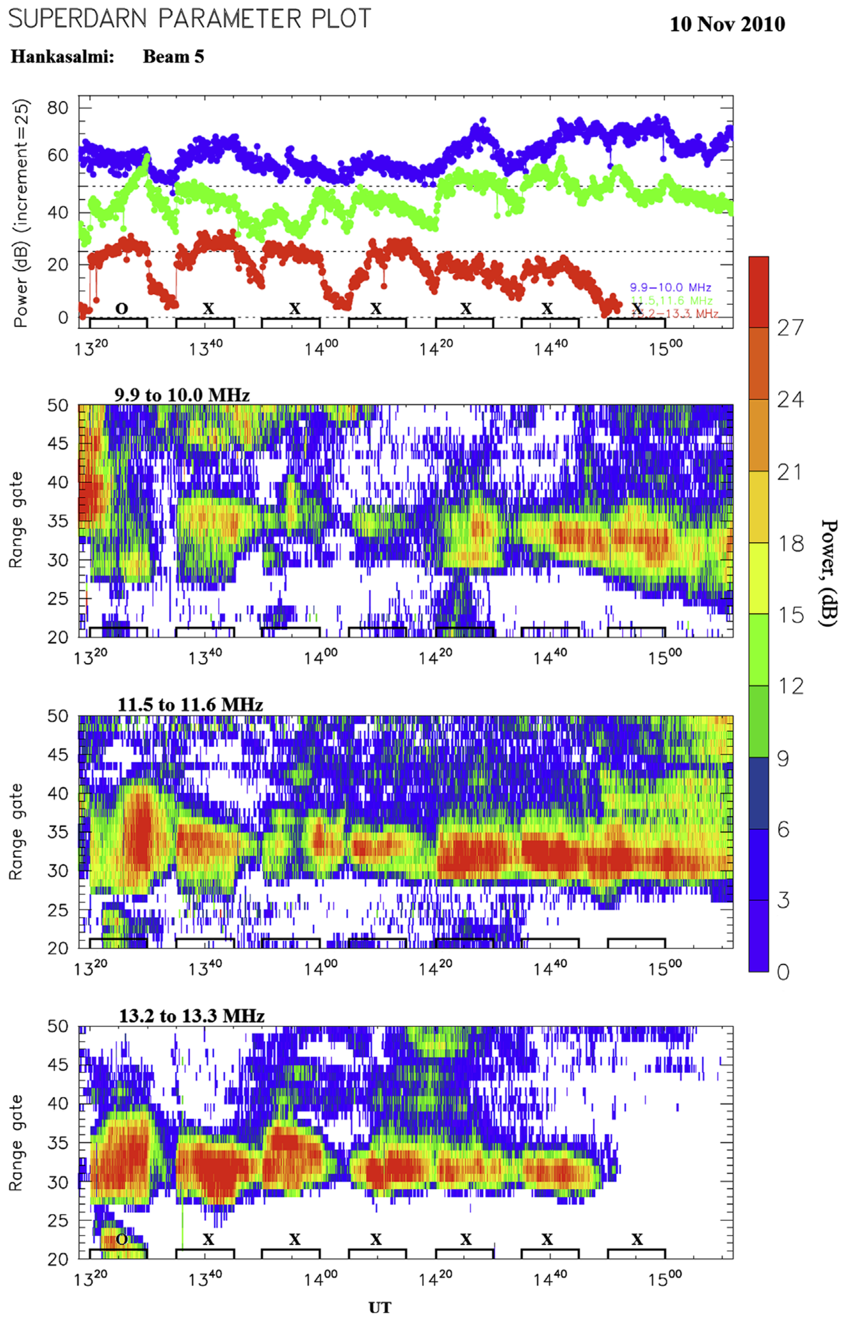

Fig. 4. Backscattered power from the Hankasalmi (Finland) CUTLASS radar (beam 5) at operational frequencies of about 10, 11.5 and 13 MHz during the experiment on 10 November 2010 from 13:18 to 15:12 UT. Behavior of the backscattered power averaged between 30–34 gates, corresponding to the central part of the heated patch, is shown in the top panel and its behavior in the range-gate –universal time UT coordinates is given in the bottom panels. The HF pump wave was radiated at a frequency of 4.544 MHz towards magnetic zenith. Effective radiated power was about 210 MW. O/X-mode heater-on periods are marked on the top panel on the time axis.

scattered signals at three CUTLASS frequencies even when the heater frequency is near the critical frequency of *F*2 layer ($f_H \approx foF2$). On 10 November 2010 X-mode heating was performed during six 10 min consecutive heating cycles (see Table 1). The excitation of AFAIs with different spatial scales, responsible for the CUTLASS backscatter, occurred in all six heater-on periods when the critical frequency of *F*2 layer dropped from 4.5 to 3.6 MHz. The growth time of X-mode AFAIs is only about 10 s, that is shorter in comparison with the other events. Their decay time is more than the duration of the heater-off period (5 min). At 15:05 UT the heater frequency was changed to f_H=4.04 MHz. Again, the excitation of X-mode AFAIs occurred in all six heater-on periods when the critical frequency of *F*2 layer dropped from 3.6 to 3.0 MHz.

Experiments on 5 and 6 March 2011 (cases 16–18 in Table 1) were carried out under disturbed conditions. In such conditions, X-mode AFAIs were also generated, when the heater frequency exceeded the value of *foF*2 by 0.2–1.2 MHz. However, signals scattered from AFAIs were observed at only one frequency ~10 MHz and they were weaker as compared with the quiet conditions.

The analysis of all events listed in Table 1 has shown that, according to data from the CUTLASS Hankasalmi radar, the spatial size of the region in the north-south direction, in which the mentioned irregularities were excited, amounted to about 75–120 km. Recall that phased array 2 of the HF heater was used, resulting in an effective radiated power (ERP) of 75–180 MW and frequencies less than 5.54 MHz. The width of the HF antenna beam at the - 3 dB point was 12°–14° depending on the heater frequency. Thus, the size of the artificially disturbed *F* region of the ionosphere, determined by the antenna pattern of phased array 2, at altitudes of 220–250 km amounts to about 60 km.

3.2. Heater-induced plasma parameter changes

During the experiments EISCAT UHF incoherent scatter data from Tromsø site measured the ionospheric plasma parameters, such as the electron density and temperature (*Ne* and *Te*), the ion temperature (*Ti*), and the ion velocity (*Vi*), in the altitude range from 90 to 600 km mostly in the direction of the magnetic zenith. The ion temperature (*Ti*) and the ion velocity (*Vi*) were either unchanged or did not change much. Hence, the UHF radar data were examined only to estimate the changes in the electron temperature (*Te*) and electron density (*Ne*) at different altitudes, induced by the powerful HF radio waves with X-mode polarization. Changes in the *Te* and *Ne* were considered for different effective radiated power (ERP). During the experiments the UHF radar measured in the magnetic field-aligned direction. The HF EISCAT Heating facility at Tromsø was running using phased array 2, resulting in ERP=75–180 MW and frequencies <5.5 MHz, and with phased array 1, resulting in ERP=370–840 MW and frequencies >5.5 MHz.

3.2.1. Effective radiated power of 75–180 MW

The results obtained for contrasting O/X –mode heating clearly demonstrate that an HF pump wave with X-mode polarization heats the ionosphere through collision processes more effectively than an O-mode HF heater wave. Note, that it is true only for ohmic heating of electrons when the O-mode HF pump wave is not reflected from the ionosphere because $f_H > foF2$ by about 0.1–1.2 MHz. In such conditions the thermal resonance instability cannot be realized and the anomalous heating of electrons at the upper hybrid resonance altitude cannot be produced.

Temporal variations of *Te* and *Ne* at different fixed altitudes during the experiment on 6 March 2010 from 15:38 to 17:00 UT are plotted in Fig. 5a and b, respectively. Note, that weak scattered signals were observed at 10 and 13 MHz during the O-mode heater-on period from 15:41 to 15:51 UT. Therefore here we observed not only pure ohmic heating. During the next three consecutive X-mode heater-on periods *Te* enhancements of up to 50% ($\sim$ 1000 K) above the background level occurred. The strongest *Te* enhancements took place at 214 km from 16:16 to 16:26 UT cycle. The electron density behavior (Fig. 5b) shows some interesting features. It is clearly seen that *Ne* increased by up to 30% at an altitude of 282 km during the X-mode heating cycles. *Ne* enhancements were also observed at 246 km, however no significant enhancements were observed at 214 km where the strongest *Te* enhancements occurred. Note that the experiment was conducted under quiet magnetic conditions, thus any *Ne* increases due to soft electron precipitation from the magnetosphere could be excluded.

The altitude profiles of the electron temperature *Te*(*h*) and electron density *Ne*(*h*) on 6 March 2010 are shown in Fig. 6a and b, respectively. The *Te*(*h*) and *Ne*(*h*) in Fig. 6a and b are plotted for different temporal intervals of the heater-on period from 15:56 to 16:06 UT, as well as for the time intervals just before and after the ionosphere heating by an X-mode high-power HF radio wave. It is seen from Fig. 6a that the *Te* enhancements were observed in the altitude range from 180 to 300 km. The *Te* maximum occurred near the reflection level of the powerful HF radio wave at an altitude of about 220 km. It was unexpected that the electron density increased by about 25% in a wide altitude range from 230 to 400 km. It is interesting to note that the altitude intervals, where enhancements of *Te* and *Ne* took place, did not coincide. Specifically, the maximum of *Te* was recorded near the reflection level of the high-power HF radio wave at an altitude of about 220 km, while the maximum increase in *Ne* took place at an altitude corresponding to about 270 km, i.e., 50 km higher than the *Te* disturbance maximum. Moreover, while *Te* returned to the unperturbed level after the end of heater-on cycle (the temporal interval 16:06–16:08 UT), the *Ne* disturbances persisted beyond 16:08 UT.

3.2.2. Effective radiated power of 370–840 MW

Dramatic changes in the behavior of the electron density and temperature were observed in the course of experiments in October 2011 when phased array 1 was used resulting in ERP=370–840 MW for frequencies >5.4 MHz. Table 2 describes the heater and ionosphere parameters for the experiments on 7, 8, 10, 11, and 12 October 2011 during which the ionosphere was modified by X-mode HF pump waves. In all events listed in Table 2, extremely strong electron density enhancements ($\sim$ 60–70%) in a wide altitude range up to the upper limit of the EISCAT UHF radar measurements (600 km) occurred. They were observed only in the magnetic field-aligned direction. There were no changes in vertical direction. The appearance of electron density enhancements in a narrow angle beam, but in a wide altitude range (ducts), was accompanied by increases in the electron temperature. In contrast to the *Ne* changes, the *Te* increases took place in a limited altitude range (mainly from 200 to 300 km).

Temporal variations of *Te* and *Ne* at different fixed altitudes during the experiment on 10 October 2011 from 14:50 to 16:30 UT (see case 3 in Table 2) are plotted in Fig. 7a and b, respectively. In this event the polarization of the HF pump wave was changed from O- to X-mode at 14:20 UT, when the heater frequency f_H=7.1 MHz was equal to the critical frequency of *F*2 layer *foF*2=7.1 MHz. During the first two heater-on periods from 14:20 to 14:30 and 14:35 to 14:45 UT the UHF radar was scanned between 90° and 78°. The duration of each position was of 5 min. It was found, that the strong *Ne* and *Te* enhancements were observed only in the magnetic field-aligned direction (78°). There were no changes in the vertical direction (90°). In the course of the experiment the critical frequency dropped and *foF*2 became about 5.7 MHz at 16:30 UT. Throughout the whole analyzed time interval the *Te* enhancements occurred at the altitudes of 200, 282, and 344 km. The strongest *Te* enhancements of up to 100% ($\sim$1500 K) above the background level took place at 200 km. The electron density behavior (Fig. 7b) shows some interesting features. It is clearly seen that *Ne* increased by up to 60%–70% at the altitudes of 282, 390, and 494 km during the X-mode heating cycles. However, no significant enhancements were observed at 200 km where the strongest *Te* enhancements occurred. The experiment was conducted under quiet magnetic conditions, thus any *Ne* increases due to soft electron precipitation from the magnetosphere could be excluded. It should be mentioned that extremely strong heater-enhanced ion and plasma lines were excited in the altitude range from 214 to 265 km in most heater-on periods, therefore it was not possible to make the correct estimations of the *Te* and *Ne* values between 214 and 265 km. In just the same way the strong enhancements in the *Te* and *Ne* occurred in the course of the experiment on 12 October 2011 from 15:20 to 16:30 UT (case 7 in Table 2). Here the heater frequency f_H=7.1 MHz was equal to the critical frequency of *F*2 layer *foF*2=7.1 MHz at 15.15 UT and then it gradually dropped to 5.7 MHz at 16:30 UT, that corresponds to changes in the extraordinary-mode critical frequency (*fxF*2) from 7.8 to 6.4 MHz. Thus, the frequency range, in which extremely strong *Ne* and *Te* enhancements occurred under X-mode heating, lies in

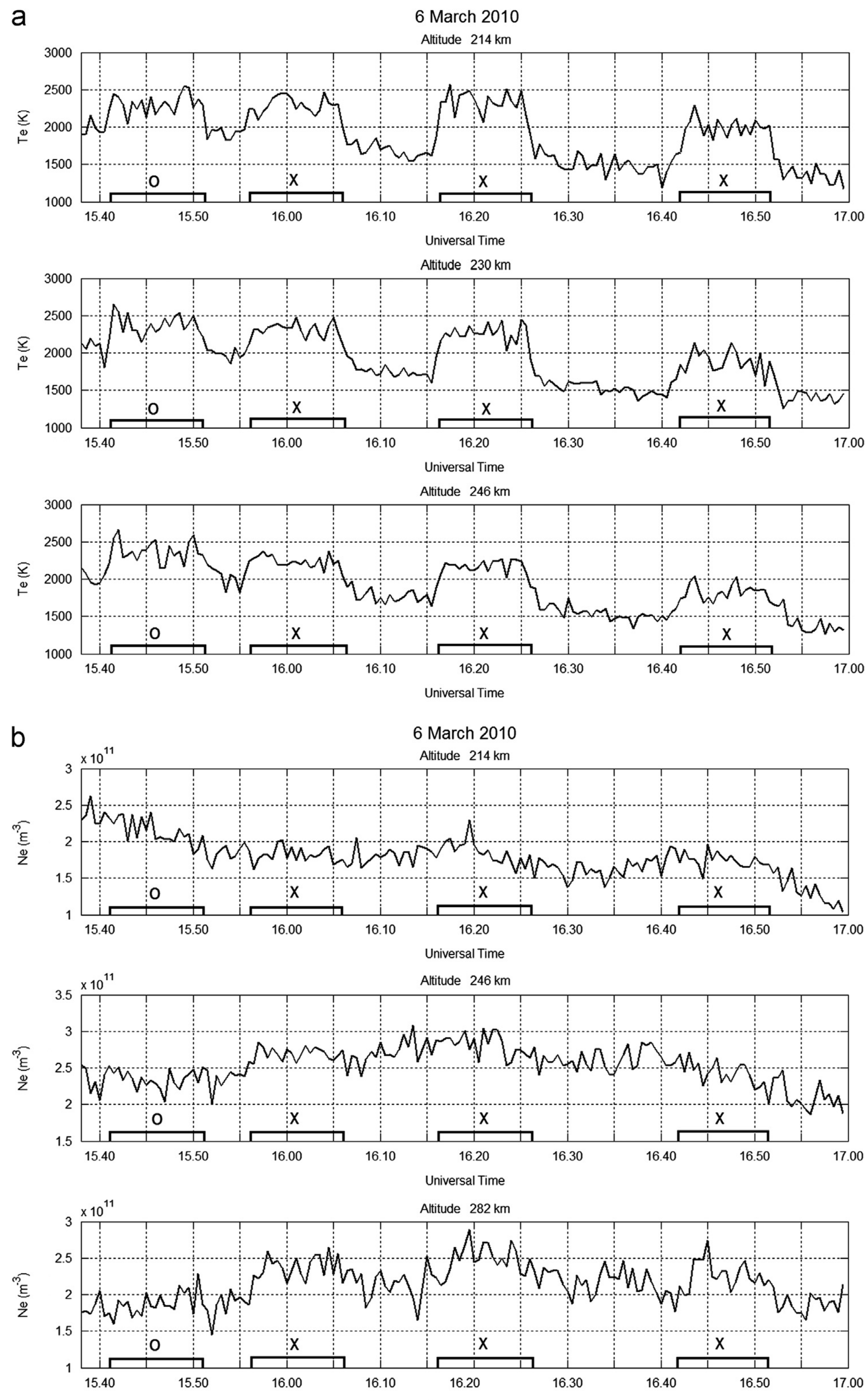

Fig. 5. Variations in time of the electron temperature *Te* (a) and electron density *Ne* (b) at different altitudes for contrasting O/X-mode heating on 6 March 2010 from 15:38 to 17:00 UT. O/X-mode heater-on periods are marked in the time axis. The HF pump wave was radiated at a frequency of 4.9128 MHz towards magnetic zenith. Effective radiated power was about 115 MW.

the interval of $f_H - f_{ce}/2 \leq fxF2 \leq f_H + f_{ce}/2$. The frequency range is bounded above by the value of the extraordinary-mode critical frequency $fxF2$ max$= f_H + f_{ce}/2$ and below by $fxF2$ min$= f_H - f_{ce}/2$. In all of the above cases listed in Table 2 the strong *Ne* and *Te* enhancements were observed when the heater frequency lies within the mentioned frequency range. Note, that in Tables 1 and 2 the values of the ordinary-mode critical frequency ($foF2$) are given. The extraordinary-mode critical frequency is determined by $fxF2 \approx foF2 + f_{ce}/2$. At Tromsø the value of the electron gyrofrequency is about $f_{ce} \approx 1.4$ MHz.

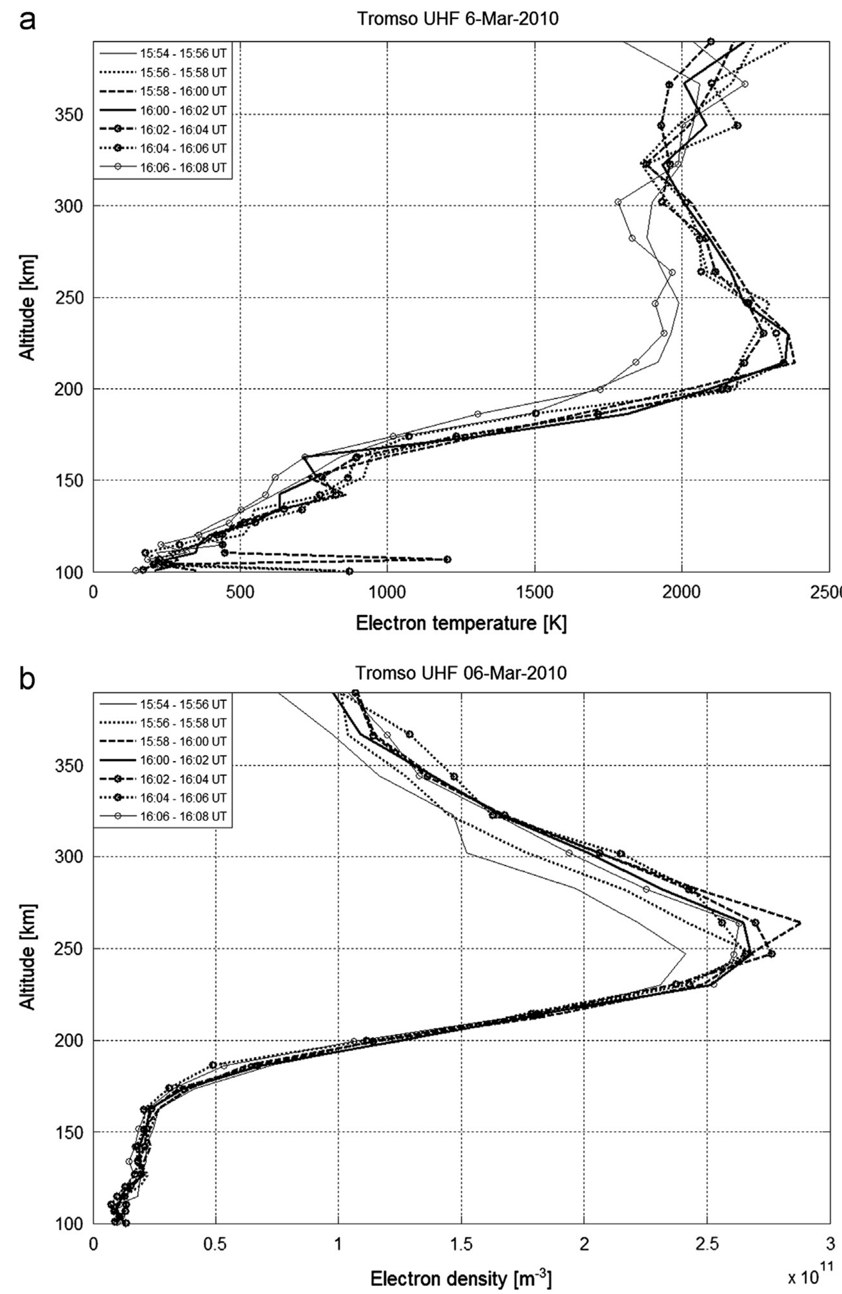

Fig. 6. Altitude profiles of the electron temperature $Te(h)$ (a) and electron density $Ne(h)$ (b) on 6 March 2010. The $Te(h)$ and $Ne(h)$ are plotted for different temporal intervals of the heater-on period from 15:56 to 16:06 UT, as well as for the time intervals just before and after the ionospheric heating by an X-mode high-power HF radio wave. The HF pump wave was radiated at a frequency of 4.9128 MHz towards magnetic zenith. Effective radiated power was about 115 MW.

The altitude profiles of the electron temperature $Te(h)$ and electron density $Ne(h)$ on 10 October 2011 are shown in Fig. 8a and b, respectively. The $Te(h)$ and $Ne(h)$ in Fig. 8a and b are plotted for different temporal intervals of the heater-on period from 14:50 to 15:00 UT, as well as for the time intervals just before and after the heater-on period. During the first two minutes of the heater-on period strong heater-enhanced ion and plasma lines were excited. Thus we did not present in Fig. 8a and b the $Te(h)$ and $Ne(h)$ for 14:50–14:52 UT. It is seen from Fig. 8a that the Te enhancements were observed in the altitude range from 200 to 300 km. The Te maximum was observed at an altitude of about 230 km. It was unexpected that the electron density increased by about 60–70% in a wide altitude range from 230 to 550 km. Again, similar to the event on 6 March 2010, the altitude intervals where enhancements of Te and Ne took place did not coincide. The maximum of Te was recorded near the reflection level of a high-power HF radio wave at an altitude of about 230 km, while the maximum enhancement in Ne took place at an altitude corresponding to about 265 km, i.e., by 35 km higher than the Te disturbance maximum.

4. Discussion

We presented experimental evidence of the excitation of strong small-scale AFAIs, with spatial scales across the geomagnetic field of the order of $l_\perp \approx$ 9–15 m, in the high-latitude F region of the ionosphere due to an X-mode HF pump wave, radiated in the

Table 2
List of the EISCAT Heating experiments when the strong *Te* and *Ne* enhancements occurred under X-mode heating of the *F* region of the high latitude ionosphere with the use of the phased array 1.

N	Date	Time of observations, (UT)	Total number of "ON" cycles	f_H, (MHz)	ERP, (MW)	*foF*2, (MHz)
1	7.10.11	16:05–17:00	4	6.77	460	6.2–5.8
2	8.10.11	14:05–15:15	5	7.953	758	7.0–6.5
3	10.10.11	14:20–16.30	9	7.1	651	7.1–5.7
4		17:20–18:30	5	5.423	371	4.8–4.1
5	11.10.11	13:50–15:45	8	7.953	839	7.7–6.7
6	12.10.11	14:50–15:15	2	7.953	836	7.3–7.1
7		15:20–16:30	5	7.1	642	7.1–5.7

direction of magnetic zenith. Their generation requires X-mode *F* region heating at frequencies, $f_{H,}$ which are above the ordinary-mode critical frequency *foF*2 by 0.1–1.2 MHz (see Table 1). The behavior and properties of such irregularities are different from AFAIs excited at the upper hybrid resonance altitude when an O-mode polarized HF pump wave is reflected from the ionosphere. From all of the above cases listed in Table 1 it was found that the X-mode AFAIs appeared 10 s–4 min after the heater is turned on. The maximum growth time was observed from the "cold" start in the first X-mode heater-on period. In the following heater-on cycles the growth time tends to decrease. The decay time of X-mode AFAIs varied in a wide range between 3 and 30 min. In some heating cycles the intensity of AFAIs stayed on the same level for 1–3 min after the heater is turned off.

The large growth and decay times observed are typical for large-scale ionospheric irregularities with spatial scales of the order of the heated patch (~60 km). In such a case one would expect that the behavior of the small-scale AFAIs, with spatial scales of the order $l_\perp \approx$ 9–15 m, which are responsible for the strong backscattered signals from the CUTLASS measurements, are driven by the large-scale ionospheric irregularities. The large-scale irregularities can be produced by the X-mode HF pump wave. The electron thermal pressure force, arising from the differential ohmic heating of electrons (Gurevich, 1978), pushes electrons to form the large-scale irregularities, which in turn break up the HF pump wave via the filamentation instability (Kuo and Schmidt, 1983). The generation of large-scale irregularities is induced by the growth of a self-focusing instability of an electromagnetic wave beam (Gurevich, 1978). One would expect that, after the HF heater is turned off, the artificial small-scale irregularities within large-scale formations are supported by a Lorentz-type mechanism suggested by Kagan (1996). The Lorentz-type forces that could result in plasma turbulence (AFAIs), might appear because of a curvature of magnetic field lines and electron inertia, as well as of the plasma pressure gradient.

The mechanism of the X-mode AFAIs is not clear. Vas'kov and Ryabova (1998) have theoretically shown that the generation process of short wavelength (upper hybrid and electron cyclotron) plasma oscillations can be produced by induced scattering of a powerful extraordinary HF radio waves by ions. They also note that the high frequency turbulence excited near the reflection level of the powerful extraordinary HF wave leads to the substantial enhancements of low frequency plasma perturbations.

The excitation of X-mode AFAIs is accompanied by the electron temperature (*Te*) and electron density (*Ne*) enhancements, depending on the effective radiated power. The maximum *Te* enhancements of up to 50% (~ 1000 K) above the background level occurred under ERP=75–180 MW, whereas they amounted up to 100% (~ 1500 K) at ERP=370–840 MW. The *Te* enhancements were mainly observed over an altitude range of about 100 km from 200 to 300 km. The X-mode HF pump wave is reflected at an altitude that is below the upper hybrid resonance layer. It cannot effectively produce anomalous heating in the *F* region. Nonetheless the X-mode pump wave heats the ionosphere through the collision process more effectively in the comparison with the O-mode heating (Kuo et al., 2010). The collisional heating process is non-local and moves the ionosphere upwards. Results obtained by Lofas et al. (2009) have shown that *F* region electron heating by X-mode radio waves in the under dense high latitude ionosphere ($f_H > foF2$) produced *Te* enhancements of the order of 300–400 K. The experiments were performed at the Tromsø HF heating facility during quiet nighttime conditions with low ionospheric densities so no reflections occurred. Numerical simulation of ohmic heating by the pump wave reproduces both altitude profiles and temporal dependence of the temperature modifications in the experiments (Lofas et al., 2009). In our X-mode heating experiments the *Te* enhancements well over 300–400 K were observed. Thus the ohmic heating is not the only factor of the *Te* enhancements.

The *Te* enhancements were accompanied by *Ne* enhancements of up to 30% over the background level under ERP=75–180 MW. These were observed over a wide altitude range from 220 to 400 km with an enhancement peak at ~270 km, which is ~50 km higher than the *Te* enhancement peak. Dramatic changes in the *Ne* behavior were observed, when phased array 1 was used resulting in ERP=520–1100 MW. Extremely strong electron density enhancements (~ 60–70%) in a wide altitude range up to the upper limit of the EISCAT UHF radar measurements (600 km) occurred. These were observed only in the magnetic field-aligned direction. Again, similar to the case of ERP=75-180 MW, the altitude intervals, where enhancements of *Te* and *Ne* took place did not coincide. The maximum *Ne* enhancement took place at an altitude of about 265 km, which is ~35 km higher than the *Te* disturbance maximum. The fact that an X-mode HF pump wave moves the ionosphere upward, can be clearly seen from experiments conducted.

The observed altitude profiles of electron density differ drastically from those typical for the O-mode heating: There was no *Ne* cave-out in the bottom of the *F*-layer, their time history shows that the *F*-layer bottom profile stayed unchanged to the altitude below of ~220 km during the X-mode heating. The electron density starts to increase from the altitude where the electron temperature reaches its maximum. *Ne* increases with X-mode heating showing no possible altitude redistribution of plasma (electrons) and indicating a possibility of triggering ionization near the X-mode reflection area. There were no significant changes in ion temperatures and velocities during the X-mode heating. The absence of increased ion velocities would rule out plasma redistribution in favor of ionization mechanisms.

Plasma density increases might result from changed temperature-dependent reaction rates, leading to transiently changed plasma density (Sipler and Biondi, 1972). Taking into account Schunk and Nagy (2000), the calculations of electron density response to increases in *Te* were performed for three altitudes of 214, 230, and 264 km with a time constant of 30 s, when increases in electron temperatures due to HF pumping effects varied from 50 to 100%. The [N2] and [O] densities for corresponding altitude were taken from the MSIS model (http://omniweb.gsfc.nasa.gov/vitmo/msis_vitmo.html). The calculations give *Ne* enhancements from 2.4 to 5.3%, depending on the altitude and the *Te* enhancements. Thus we conclude that observed *Ne* enhancements under X-mode HF heating cannot be explained by temperature-dependent reaction rates. Enhanced production of ionization by accelerated electrons is an alternative mechanism for *Ne* increases induced by an X-mode heating. Carlson (1993) proposed the production of ionization by accelerated electrons, and presented calculations showing that the observable plasma density enhancements, provided by the efficient conversion of HF

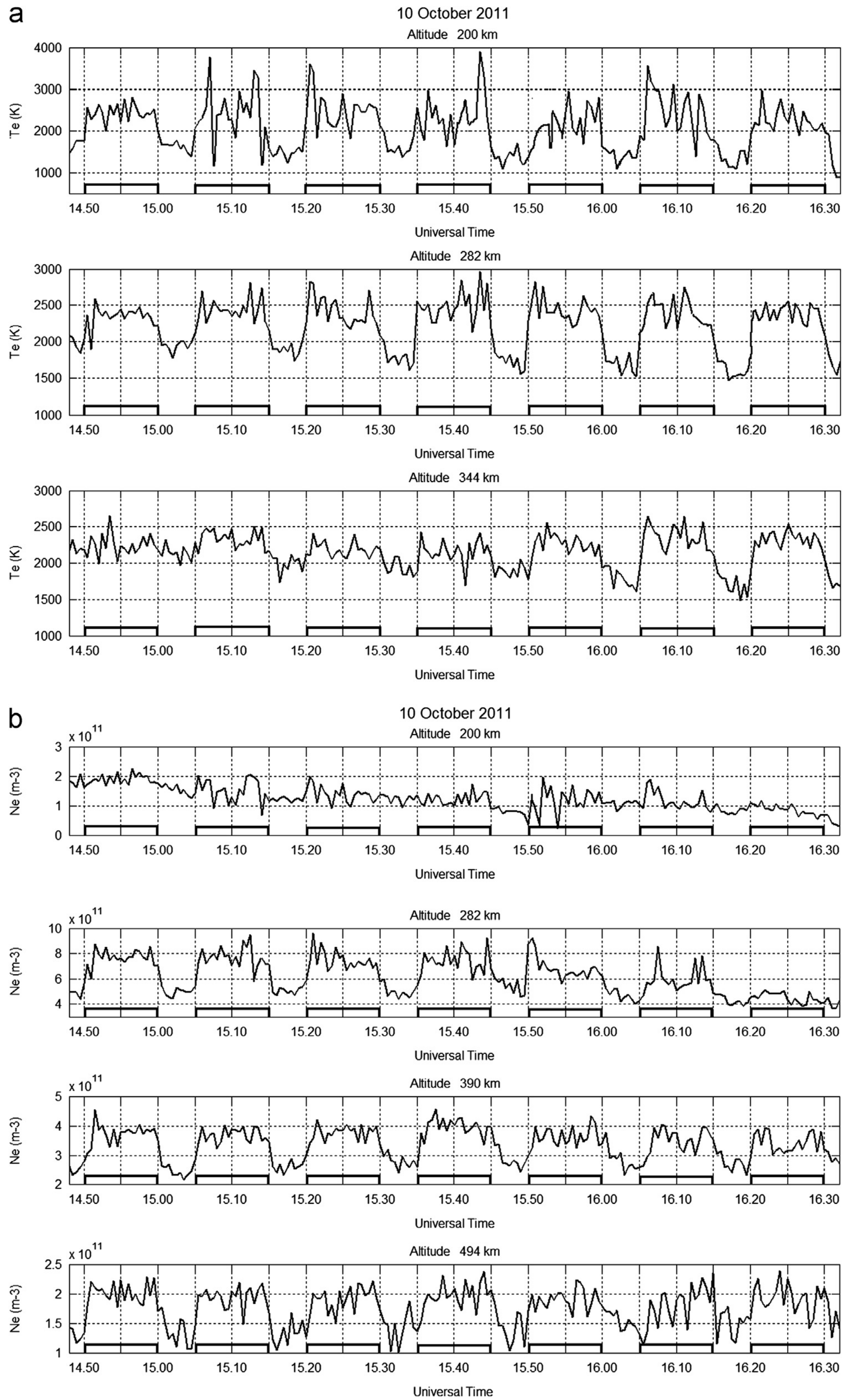

Fig. 7. Variations in time of the electron temperature *Te* (a) and electron density *Ne* (b) at different altitudes for X-mode heating on 10 October 2011 from 15.38 to 17.00 UT. The X-mode heater-on periods are marked on the time axis. The HF pump wave was radiated at a frequency of 7.1 MHz towards magnetic zenith. Effective radiated power was about 651 MW.

energy to the electron flux energy, can occur when enough ERP is transmitted.

From all experimental data obtained, the frequency window, in which AFAIs, *Ne* and *Te* enhancements occurred under X-mode heating, can be defined. It lies in the frequency range $f_H - f_{ce}/2 \leq fxF2 \leq f_H + f_{ce}/2$, where f_{ce} is the electron gyrofrequency. The frequency range is bounded above by the value of the extraordinary-mode critical frequency $fxF2max = f_H + f_{ce}/2$ and

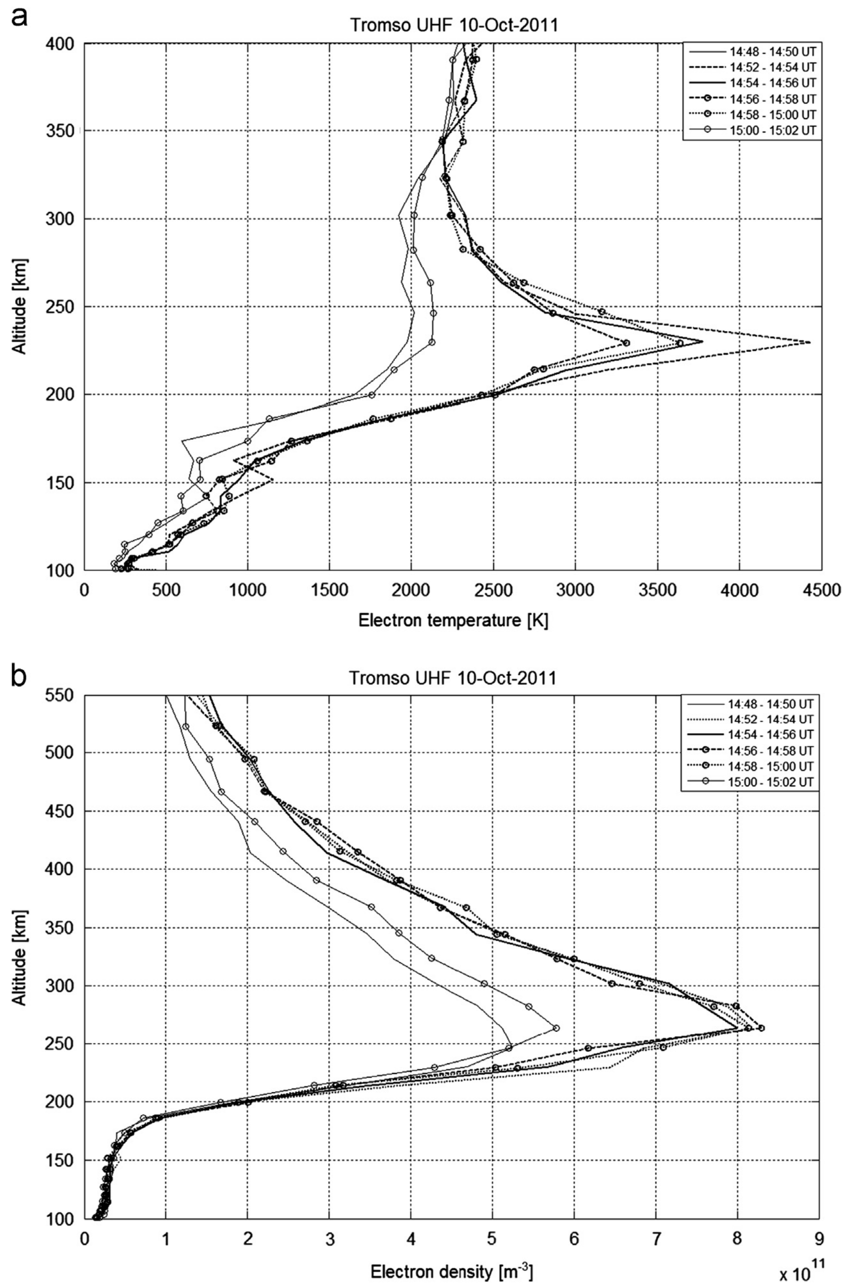

Fig. 8. Altitude profiles of the electron temperature $Te(h)$ (a) and electron density $Ne(h)$ (b) on 10 October 2011. The $Te(h)$ and $Ne(h)$ are plotted for different temporal intervals of the heater-on period from 14:50 to 15:00 UT, as well as for the time intervals just before and after the ionospheric heating by an X-mode high-power HF radio wave. The HF pump wave was radiated at a frequency of 7.1 MHz towards magnetic zenith. Effective radiated power was about 651 MW.

below by $fxF2\text{min}=f_H-f_{ce}/2$. In all of the above cases listed in Tables 1 and 2 strong AFAIs, *N*e and *T*e enhancements were observed, when the heater frequency lies within the mentioned frequency window.

What are the electron acceleration mechanisms leading to the *N*e enhancements during X-mode HF heating? We have to mention that the EISCAT UHF radar spectra during X-mode HF pumping demonstrate strongly heater-enhanced ion-acoustic and plasma lines, which are unusual for X-mode heating. These heater-enhanced ion and/or plasma line backscatter enhancements are typical signatures of parametric decay instability. It is known (Stubbe, 1996; DuBois et al., 1990) that an electromagnetic O-mode HF pump wave EM_O at the reflection altitude decays into plasma Langmuir (L) and ion-acoustic (IA) waves, $EM_O \rightarrow L+IA$. These electrostatic plasma waves (L and IA) propagate near –parallel to the magnetic field direction. Langmuir turbulence near the pump reflection height can lead to the generation of fluxes of accelerated electrons and enhanced production of ionization (see, for example, Carlson, 1993; Gurevich et al., 2004; Mishin et al., 2004). An X-mode HF pump wave cannot excite Langmuir waves. The electric field of the X-mode pump wave is perpendicular to the magnetic field. On the other hand, Langmuir waves are mainly polarized in the magnetic field direction. We assume that there is some evidence that the X- mode wave may first be converted to the Z- mode, which can then propagate above the X-mode reflection altitude. Intense plasma turbulence may be generated by $Z \rightarrow L$ (Mjolhus and Fla, 1984) independent of how far the heater frequency f_H is away from a gyroharmonic. In such a case the conversion process, as $X - Z \rightarrow L+IA$, could be realized. It should be mentioned that during our experiments there is an evidence for simultaneous production of AFAIs and IA and L waves, which were observed throughout the whole heater-on period. Thus we suggest, in addition to processes involving direct electrostatic conversion of the Z-mode wave, that Z-mode waves can be scattered by AFAIs. In turn, it can lead to the production of outshifted plasma lines (Mishin et al., 1997; Mishin et al., 2001). Langmuir turbulence excited by this way is an alternative mechanism for electron acceleration.

5. Summary

The results, obtained from numerous X-mode HF pumping experiments in the high-latitude *F* region of the ionosphere, have shown an evidence of the excitation of strong small-scale AFAIs, with spatial scales across the geomagnetic field of the order of $l_{\perp} \approx 9$–15 m. Their generation requires X-mode *F* region heating at frequencies above the ordinary-mode critical frequency *foF*2 by 0.1–1.2 MHz. It was found that the X-mode AFAIs appeared 10 s–4 min after the heater is turned on. The maximum growth time was observed from the "cold" start in the first X-mode heater-on period. In the following heater-on cycles the growth time tends to decrease. The decay time of X-mode AFAIs varied in a wide range between 3 and 30 min. In some heating cycles the intensity of AFAIs stayed on the same level during 1–3 min after the heater is turned off. It is expected that the behavior of the small-scale AFAIs, responsible for the strong backscattered signals from the CUTLASS measurements is driven by the large-scale ionospheric irregularities.

The excitation of X-mode AFAIs is accompanied by electron temperature (*T*e) and electron density (*N*e) enhancements depending on the effective radiated power (ERP). The maximum *T*e enhancements of up to 50% (~1000 K) above the background level occurred under ERP=75–180 MW, whereas they amounted up to 100% (~1500 K) for ERP=370–840 MW. Such strong electron heating suggests that the ohmic heating is not the only factor of the *T*e enhancements.

The *T*e enhancements were accompanied by *N*e enhancements of up to 30% over the background level under ERP=75–180 MW. Unexpected strong electron density enhancements (~60–70%) in a wide altitude range up to the upper limit of the EISCAT UHF radar measurements (600 km) occurred at ERP=370–840 MW. The altitude intervals, where enhancements of *T*e and *N*e took place did not coincide. The maximum *N*e enhancement took place at an altitude which is ~35–50 km higher than the *T*e disturbance maximum.

It was found that AFAIs, *N*e and *T*e enhancements occurred, when the extraordinary-mode critical frequency (*fxF*2) lies in the frequency range $f_H - f_{ce}/2 \le fxF2 \le f_H + f_{ce}/2$,.

It was shown that observed *N*e enhancements under X-mode HF heating cannot be explained by temperature-dependent reaction rates. Enhanced production of ionization by accelerated electrons is an alternative mechanism for *N*e increases induced by an X-mode heating. Fluxes of accelerated electrons can be produced by Langmuir turbulence. Taking into account that an X-mode wave cannot produce the Langmuir waves, we assume that the X-mode may first be converted to the Z- mode, which can induce intense plasma turbulence above the X-mode reflection altitude. In addition to processes involving direct electrostatic conversion of the Z-mode wave, the Z-mode waves can be scattered by AFAIs that, in turn, can also lead to the producing Langmuir turbulence.

Acknowledgments

We would like to thank the EISCAT Scientific Association for providing the Tromsø heating experiments in conjunction with the EISCAT UHF radar measurements. CUTLASS is supported by the UK Science and Technology Facilities Council Grant PP/E007929/1, the Finnish Meteorological Institute, and the Swedish Institute of Space Physics. TKY is supported by the Science and Technology Facilities Council Grant ST/H002480/1. Authors are thankful to Reviewer 2 for useful comments and suggestions.

References

Blagoveshchenskaya, N.F., 2001. Geophysical phenomena in the near Earth space environment initiated by active experiments. Gidrometizdat. St. Petersburg (in Russian).

Blagoveshchenskaya, N.F., Kornienko, V.A., Petlenko, A.V., Brekke, A., Rietveld, M.T., 1998. Geophysical phenomena during an ionospheric modification experiment at Tromsø. Annales Geophysicae 16, 1212–1225.

Blagoveshchenskaya, N.F., Borisova, T.D., Kornienko, V.A., Leyser, T.B., Rietveld, M.T., Thide, B., 2006. Artificial field-aligned irregularities in the nightside auroral ionosphere. Advances in Space Research 38, 2503–2510.

Blagoveshchenskaya, N.F., Carlson, H.C., Kornienko, V.A., Borisova, T.D., Rietveld, M.T., Yeoman, T.K., Brekke, A., 2009. Phenomena induced by powerful HF pumping towards magnetic zenith with a frequency near the F-region critical frequency and the third electron gyro harmonic frequency. Annales Geophysicae 27, 131–145.

Blagoveshchenskaya, N.F., Borisova, T.D., Yeoman, T., Rietveld, M.T., Ivanova, I.M., Baddeley, L.J., 2011a. Artificial field-aligned irregularities in the high-latitude F region of the ionosphere induced by an X-mode HF heater wave. Geophysical Research Letters, 38, http://dx.doi.org/10.1029/2011GL046724.

Blagoveshchenskaya, N.F., Borisova, T.D., Yeoman, T.K., Rietveld, M.T., 2011b. The effects of modification of a high-latitude ionosphere by high-power HF radio waves. Part 1. Results of multi-instrument ground-based observations. Radiophysics and Quantum Electronics (English Translation) 53 (9–10), 512–531.

Carlson, H.C., 1993. High power HF modification: Geophysics, span of EM effects, and energy budget. Advances in Space Research 13 (10), 15–24.

Djuth, F.T., Jost, R.J., Noble, S.T., Gordon, W.E., Stubbe, P., Kopka, H., Nielsen, E., Bostrom, R., Derblom, H., Hedberg, A., Thide, B., 1985. Observations of E region irregularities generated at auroral latitudes by a high power radio wave. Journal of Geophysical Research 90, 12293–12306.

DuBois, D.F., Rose, H.A., Russell, D., 1990. Excitation of strong Langmuir turbulence in plasmas near critical density: application to HF heating of the ionosphere. Journal of Geophysical Research 95, 21221–21272.

Eglitis, P., Robinson, T.R., Rietveld, M.T., Wright, D.M., Bond, G.E., 1998. The phase speed of artificial field-aligned irregularities observed by CUTLASS during HF modification of the auroral ionosphere. Journal of Geophysical Research 103, 2253–2259.

Frolov, V.L., Erukhimov, L.M., Metelev, S.A., Sergeev, E.N., 1997. Temporal behavior of artificial small-scale ionospheric irregularities: review of experimental results. Journal of Atmospheric and Solar-Terrestrial Physics 59, 2317–2333.

Frolov, V.L., Kagan, L.M., Sergeev, E.N., Komrakov, G.P., Bernhardt, P.A., Goldstein, J.A., Wagner, L.S., Selcher, C.A., Stubbe, P., 1999. Ionospheric observations of F region artificial plasma turbulence, modified by powerful X-mode radio waves. Journal of Geophysical Research 104 (A6), 12695–12704.

Grach, S.M., Trakhtengerts, V.Y., 1976. Parametric excitation of ionospheric irregularities extended along the magnetic field line. Radiophysics and Quantum Electronics (English Translation) 18, 951–957.

Greenwald, R.A., Baker, K.B., Dudeney, J.R., et al., 1995. DARN/SuperDARN: a global view of the dynamics of high-latitude convection. Space Science Review 71, 761–796.

Gurevich, A.V., 1978. Nonlinear Phenomena in the Ionosphere. Springer-Verlag, New York.

Gurevich, A.V., 2007. Nonlinear effects in the ionosphere. Physics–Uspekhi (English Translation) 50, 1091–1121.

Gurevich, A.V., Carlson, H.C., Medvedev, Yu.V., Zybin, K.R., 2004. Langmuir turbulence in ionospheric plasma. Plasma Physics Reports 30, 995–1005.

Hedberg, A., Derblom, H., Thide, B., Kopka, H., Stubbe, P., 1983. Observations of HF backscatter associated with the heating experiment at Tromso. Radio Science 18, 840–850.

Honary, F., Robinson, T.R., Wright, D.M., Stocker, A.J., Rietveld, M.T., McCrea, I., 1999. First direct observation of the reduced striations at pump frequencies close to the electron gyroharmonics. Annales Geophysicae 17, 1235–1238.

Hysell, D.L., Kelley, M.C., Yampolski, Y.M., Beley, V.S., Koloskov, A.V., Ponomarenko, P.V., Tyrnov, O.F., 1996. HF radar observations of decaying artificial field-aligned irregularities. Journal of Geophysical Research 101, 26981–26993.

Kagan, L.M., 1996. A Lorentz-type mechanism for generation of small-scale irregularities in the heater-modified ionosphere. Radiophysics and Quantum Electronics (English Translation) 393 (3), 318–328.

Kelley, M.C., Arce, T.L., Salowey, J., Sulzer, M., Armstrong, W.T., Carter, M., Duncan, L., 1995. Density depletions at the 10 m scale induced by the Arecibo heater. Journal of Geophysical Research 100, 17367–17376.

Kuo, S.P., Schmidt, G., 1983. Filamentation instability in magneto plasmas. Physics Fluids 26, 2529–2536.

Kuo, S., Cheng, W.-T., Snyder, A., Kossey, P., Battis, J., 2010. Contrasting O/X-mode heater effects on O-mode sounding echo and the generation of magnetic pulsations. Geophysical Research Letters 37, L01101, http://dx.doi.org/10.1029/2009GL041471.

Lester, M., Chapman, P.J., Cowley, S.W.H., et al., 2004. Stereo CUTLASS: A new capability for the SuperDARN radars. Annales Geophysicae 22, 459–473.

Lofas, H., Ivchenko, N., Gustavsson, B., Leyser, T.B., Rietveld, M.T., 2009. F-region electron heating by X-mode radiowaves in under dense conditions. Annales Geophysicae 27, 2585–2592.

Minkoff, J., Kugelman, P., Weissman, I., 1974. Radio frequency scattering from a heated ionospheric volume, 1, VHF/UHF field-aligned and plasma-line backscatter measurements. Radio Science 9, 941–955.

Mishin, E., Hagfors, T., Kofman, W., 1997. On origin of outshifted plasma lines during HF modification experiments. Journal of Geophysical Research 102, 27265–27269.

Mishin, E., Hagfors, T., Isham, B., 2001. A generation mechanism for topside enhanced incoherent backscatter during high frequency modification experiments in Tromsø. Geophysical Research Letters 28, 479–482.

Mishin, E.V., Burke, W.J., Pedersen, T., 2004. On the onset of HF induced airglow at HAARP. Journal of Geophysical Research 109, A02305, http://dx.doi.org/10.1029/2003JA010205.

Mjolhus, E., Fla, T., 1984. Direct access to plasma resonance in ionospheric radio experiments. Journal of Geophysical Research 89, 3921–3928.

Noble, S.T., Djuth, F.T., Jost, R.J., Gordon, W.E., Hedberg, A., Thide, B., Derblom, H., Bostrom, R., Nielsen, E., Stubbe, P., Kopka, H., 1987. Multiple frequency radar observations of high-latitude E region irregularities in the HF modified ionosphere. Journal of Geophysical Research 92, 13613–13627.

Rietveld, M.T., Kohl, H., Kopka, H., Stubbe, P., 1993. Introduction to ionospheric heating at Tromsø–I. Experimental overview. Journal of Atmospheric and Solar-Terrestrial Physics 55, 577–599.

Rietveld, M.T., Kosch, M.J., Blagoveshchenskaya, N.F., Kornienko, V.A., Leyser, T.B., Yeoman, T.K., 2003. Ionospheric electron heating, aurora and striations induced by powerful HF radio waves at high latitudes: aspect angle dependence. Journal of Geophysical Research 108 (A4), 1141, http://dx.doi.org/10.1029/2002JA009543.

Rishbeth, H., van Eyken, T., 1993. EISCAT: Early history and the first ten years of operation. Journal of Atmospheric and Solar-Terrestrial Physics 55, 525–542.

Robinson, T.R., Stocker, A.J., Bond, G.E., Eglitis, P., Wright, D.M., Jones, T.D., 1997. O-and X-mode heating effects observed simultaneously with the CUTLASS and EISCAT radars and low power HF diagnostic at Tromsø. Annales Geophysicae 15, 134–136.

Robinson, T.R., Stocker, A.J., Bond, G.E., Eglitis, P., Wright, D.M., Jones, T.B., Rietveld, M.T., 1998. First CUTLASS-EISCAT heating results. Advances in Space Research 21, 663–666.

Robinson, T.R., Yeoman, T.K., Dhillon, R.S., Lester, M., Thomas, E.C., Thornhill, J.D., Wright, D.M., van Eyken, A.P., McCrea, I.W., 2006. First observations of SPEAR-induced artificial backscatter from CUTLASS and the EISCAT Svalbard radars. Annales Geophysicar 24, 291–309.

Schunk, R.W., Nagy, A.F., 2000. Ionospheric physics, plasma physics, and chemistry. Cambridge University Press.

Sipler, D.P., Biondi, A., 1972. Measurements of O (^{1}D) quenching rates in the F region. Journal of Geophysical Research 77 (6202–6218), 1972.

Stubbe, P., 1996. Review of ionospheric modification experiments at Tromso. Journal of Atmospheric and Solar-Terrestrial Physics 58, 349–368.

Vas'kov, V.V., Gurevich, A.V., 1976. Nonlinear resonant instability of a plasma in the field of an ordinary electromagnetic wave. Soviet Physics JETP (English Translation) 42, 91–97.

Vas'kov, V.V., Ryabova, N.A., 1998. Parametric excitation of high frequency plasma oscillations in the ionosphere by a powerful extraordinary radio wave. Advances in Space Research 21, 697–700.

Yampolski, Y.M., Beley, V.S., Kasheev, S.B., Koloskov, A.V., Somov, V.G., Hysell, D.L., Isham, B., Kelley, M.C., 1997. Bistatic HF radar diagnostic induced field-aligned irregularities. Journal of Geophysical Research 102 (A4), 7461–7467.

Yeoman, T.K., Blagoveshchenskaya, N.F., Kornienko, V.A., Robinson, T.R., Dhillon, R.S., Wright, D.M., Baddeley, L.J., 2007. SPEAR: Early results from a very high latitude ionospheric heating facility. Advances in Space Research 40, 384–389.